Geoheritage (2024) 16:24
https://doi.org/10.1007/s12371-024-00928-y

ORIGINAL ARTICLE

The Relationships Between Danxia Geoheritages and Regional Tectonics in Southern Sichuan Basin: Implications for the Spatial Distribution of Danxia Landforms in China

Jun-Ting Qiu[1] · Hong-Xu Mu[1] · Xin-Min Rui[1] · Yan-Jie Yang[1] · Pengju Li[2] · Liang Qiu[3] · Chao-Bin Xu[4]

Received: 10 April 2023 / Accepted: 22 January 2024 / Published online: 13 February 2024

Abstract
The Danxia geoheritage has emerged as a compelling subject of study, while the Tethys-Himalayan tectonic domain continues to captivate scholarly attention. However, a noteworthy gap exists in the literature concerning the intricate relationship between Danxia formation and the evolution of regional tectonics. In this study, we conducted a comprehensive analysis involving structure interpretation and terrain assessment, utilizing Landsat8 imagery and ASTER Global Digital Elevation Model. Additionally, field investigations were carried out on 35 Danxia landforms in the southern Sichuan Basin. Our findings revealed four distinct types of Danxia heritages—cliff (32 sites), peak (7 sites), cave (5 sites), and valley (6 sites)—with a predominant presence on slopes exceeding 40°. Moreover, valley-type sites exhibited a propensity for development at altitudes surpassing 400 m. The observed formations were intricately linked to Late Jurassic to Cretaceous red beds, influenced by the synergistic effects of the southward thrusting of the Qinling Orogen and the northwestward expansion of the Jiangnan Orogen. The control exerted by Cenozoic faults, folds, and joints—resulting from the eastward expansion of the Tibetan Plateau and the southeastward extrusion of the Chuandian terrane—further shaped these Danxia landscapes. Notably, the eastward expansion of the Tibetan Plateau induced the Cenozoic uplift of the southern Sichuan Basin, initiating a rapid denudation process of red beds crucial to the formation of Danxia landforms. Consequently, the Tethys-Himalayan tectonic evolution not only provided the material and structural foundations for these formations but also exerted a profound influence on their development in the southern Sichuan Basin. This study significantly contributes to our enhanced understanding of the spatial distribution of Danxia landforms in China.

Keywords Danxia · Jurassic and Cretaceous · Sichuan Basin · Tethys-Himalayan · Tectonic evolution

✉ Liang Qiu
qiul@cugb.edu.cn

Jun-Ting Qiu
midimyself@126.com

[1] National Key Laboratory of Science and Technology On Remote Sensing Information and Image Analysis, Beijing Research Institute of Uranium Geology, Beijing 100029, China

[2] School of Economics, Sichuan University of Science & Engineering, Zigong 643002, China

[3] State Key Laboratory of Geological Processes and Mineral Resources, School of Earth Sciences and Resources, China University of Geosciences, Beijing 100083, China

[4] Fujian Provincial Key Laboratory for Plant Eco-Physiology, School of Geographical Sciences, School of Carbon Neutrality Future Technology, Fujian Normal University, Fuzhou 350007, China

Introduction

The term “geoheritage” was initially defined by Brocx and Semeniuk (2007) to denote intrinsically or culturally significant geological sites providing insights into Earth’s evolution, applicable in research, teaching, or referential contexts. The Danxia geoheritage has become a focal point of interest (e.g., Chen 1984; Liu 1986; Liu and Huang 1991; Peng 2000; Jiang et al. 2009; Zhu et al. 2010; Li et al. 2013; Xu et al. 2013; Qiu et al 2015; Chen et al. 2022; Li et al. 2022; Shi et al. 2022; Shu et al. 2022; Jia et al. 2023), particularly intriguing due to its concentration in three primary areas in China: the South China region, the Sichuan Basin, and the Qilian-Liupan regions (Yan et al. 2019; Fig. 1). This study seeks to address the scientific inquiry of why these Danxia landforms are clustered together and whether there exists a genetic link among them.

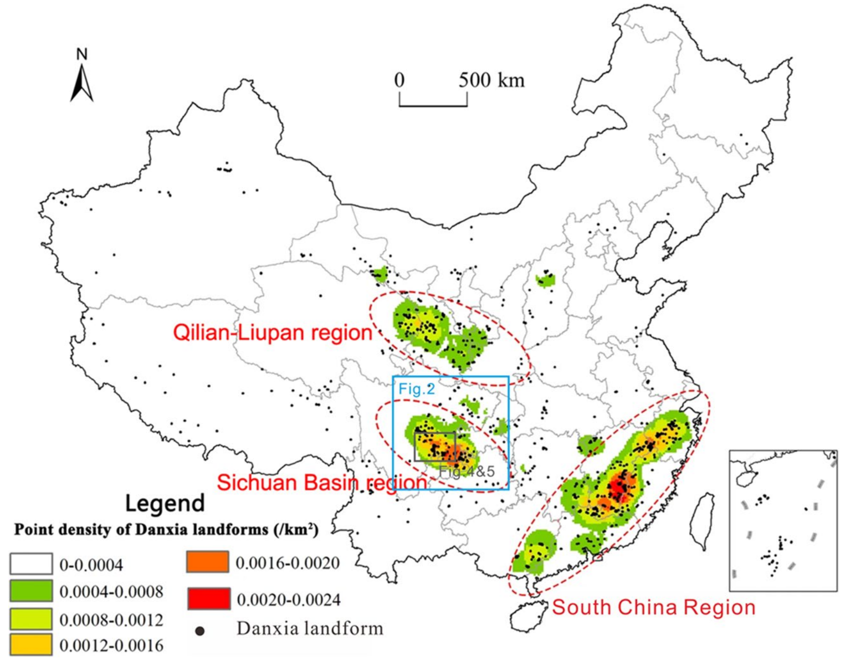

Fig. 1 Distribution of Danxia landforms in China with point densities (modified after Yan et al. 2019)

The Sichuan Basin, situated in the western portion of the Yangtze Block, is an intracontinental sedimentary basin that has undergone multiple tectonic changes influenced by both trans-Eurasian Tethys and circum-Pacific tectonics (e.g., Yan et al. 2018; Yan and Qiu 2020). While numerous studies have explored Danxia landforms in the Sichuan Basin, the majority have focused on tourism, education, and landform preservation (e.g., Guo et al 2008; Luo and Wang 2015; Qiu et al. 2015). Conversely, literature concerning tectonic evolution has predominantly emphasized geodynamics, regional metallogeny, and oil–gas storage/destruction effects (e.g., Jia et al. 2006; Liu et al. 2018). Notably, the genesis of Danxia landforms in the Sichuan Basin and its connection to regional tectonic evolution remain inadequately addressed.

The formation of Danxia landforms is commonly associated with red bed deposition, post-depositional structural activity, and subsequent erosion following red bed uplift (Ren 2009; Jiang et al. 2009, 2013; Zhu et al. 2009; Chen et al. 2019; Peng et al. 2020, 2023; Wang 2021; Li et al. 2023; Yang et al. 2023; Zhang et al. 2023). Various methods have been proposed to comprehensively understand the Danxia formation process, such as microscopic observation (Jiang et al. 2013; Wang 2021) for investigating depositional environments, geometry (Ren 2009; Chen et al. 2019; Peng et al. 2020; Li et al. 2023) and remote sensing imagery (Yang et al. 2023; Zhang et al. 2023) analyses for discerning tectonic stress field characteristics and erosion degrees, and isotopic dating (Zhu et al. 2009; Peng et al. 2023) for studying the geochronology of structural activity.

In this study, we collected and utilized ASTER Global Digital Elevation Model (ASTER GDEM) and Landsat8 images covering the southern Sichuan Basin for terrain analysis and regional structure interpretation. Additionally, field investigations were conducted on 35 Danxia landforms to comprehend their types and spatial distribution in the region. Geometry characteristics of joints associated with the Danxia landforms were measured to analyze the tectonic stress field. The results were then employed to discuss the relationship between Danxia landform formation and regional tectonic evolution. This achievement significantly contributes to a nuanced understanding of the spatial distribution of Danxia landforms in China.

Background

Regional Geology

The Sichuan Basin, situated in the western part of the South China Block, is surrounded by distinct geological features, including the Qinling Orogen to the north (Meng and Zhang 2000; Dong et al. 2011), the Daliangshan Fold Belt to the south, the Longmenshan-Daliangshan Fold-and-Thrust Belts to the west (Roger et al. 2010), and the Qiyaoshan Fold–Thrust Belt to the southeast (Fig. 2). Over geological time, it transformed from a passive continental margin into a foreland basin during the Triassic to Cretaceous era, subsequently undergoing exhumation and structural modification in the Cenozoic (Sun et al. 2018; Mu et al. 2019). Comprising both a sedimentary basement and cover, the cover primarily consists of Palaeozoic and middle Mesozoic strata characterized by shallow marine deposits and younger terrestrial strata.

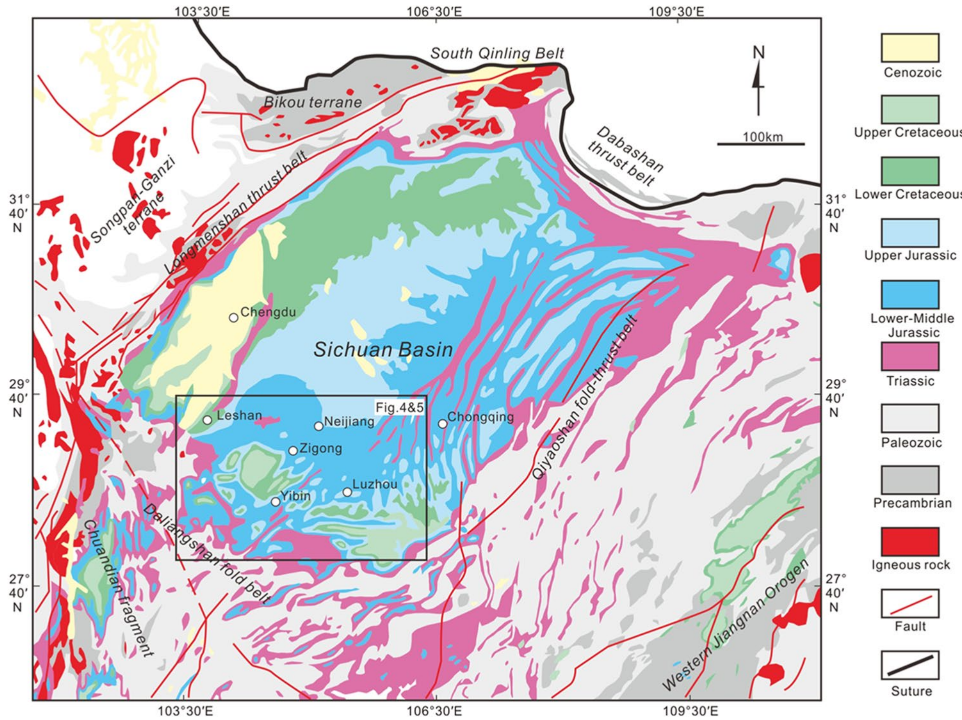

Fig. 2 Geological map delineating the distribution of Jurassic to Cretaceous strata and major terranes (modified after Li et al. 2018)

The Triassic strata, distributed along the Huayinshan fault, include the Feixianguan (T_1f), Jialingjiang (T_1j), Leikoupo (T_2l), and Xujiahe (T_3x) Formations. The Feixianguan (T_1f) Formation comprises crystalline debris tuff and shale intercalated with sandstone and limestone. The Jialingjiang (T_1j) Formation is predominantly composed of limestone and dolomite intercalated with mudstone, siltstone, and tuff. The Leikoupo (T_2l) Formation consists of dolomite intercalated with dolomitic mudstone and gypsum-salt rock. The Xujiahe (T_3x) Formation contains feldspar quartz sandstone intercalated with mud shale.

The Jurassic strata, widespread in the southern Sichuan region, include the Zhenzhuchong (J_1z), Ziliujing (J_1zl), Xintiangou (J_2x), Shaximiao (J_2s), Suining (J_3s), and Penglaizhen (J_3p) Formations. The Zhenzhuchong (J_1z) and Ziliujing (J_1zl) Formations are primarily composed of mudstone with minor quartz sandstone. The Xintiangou (J_2x) Formation consists of quartz sandstone with minor mudstone. The Shaximiao (J_2s) Formation contains mudstone and feldspar quartz sandstone. The Suining (J_3s) Formation is composed of calcareous mudstone intercalated with feldspar quartz sandstone. The Penglaizhen (J_3p) Formation comprises feldspar quartz sandstone and calcareous mudstone.

The Cretaceous strata consist of the Wotoushan (K_1w), Daerdang (K_1d), Sanhe (K_2s), and Gaokanba (K_2g) Formations. The Wotoushan Formation (K_1w) comprises feldspar quartz sandstone intercalated with mudstone. The Daerdang (K_1d) Formation is characterized by massive feldspar quartz sandstone. The Sanhe (K_2s) Formation consists of argillaceous detritus feldspar sandstone and mudstone. The Gaokanba (K_2g) Formation is dominated by fine to silty feldspar sandstone intercalated with mudstone (Li et al. 2018; Liu et al. 2021a, b).

Danxia Landforms in Southern Sichuan Basin

The Danxia landforms discovered, undergoing development, and currently operational are comprehensively detailed in Table 1, with corresponding photos and locations presented in Figs. 3 and 4, respectively. The southern Sichuan Basin encompasses five cities—Yibin, Leshan, Luzhou, Zigong, and Neijiang. Among these, Yibin, Leshan, and Luzhou stand out with a wealth of Danxia resources, featuring renowned sites like Sunanzhuhai, Leshan Giant Buddha, Huangjinglaolin, Tianxiandong, Fobao, Danshan, Huagaoxi, Qidonggou, Baxianshan, Muchuanzhuhai, and Huatianjiudi. Additionally, ongoing development efforts focus on sites such as Danshanbishui, Shiguhongyanwo, Mabiandanxia, and Biyunshan. The Zigong, while boasting numerous Danxia resources like Feilongxia and Jinhuasuoluogu, does not enjoy the same level of fame as Yibin, Leshan, and Luzhou. Conversely, Neijiang exhibits a scarcity of prominent Danxia resources, with the Daxia resource presence being notably limited in comparison to other cities in the region.

Table 1 The Danxia landforms in the southern Sichuan Basin

City	County	Name
Yibin	Changning	Shunanzhuhai
		Qidonggou
	Gaoxian	Kejiuhongyanshan
		Shengtianhongyanshan
	Nanxi	Guankou
		Yuntaishan
	Cuiping	Danshanbishui
		Shiguhongyanwo
		Huishigou
		Longtoushan
	Jiangan	Renhebaizhuhai
	Pingshan	Baxianshan
	Xuzhou	Shichengshan
Leshan	Shizhong	Leshan Giant Buddha
		Pingqiangxiaosanxia
	Muchuan	Muchuanzhuhai
		Liaoqingyan
	Jiajiang	Qianfoyan
		Biyunshan
	Jianwei	Yunfengshan
		Ziyunshan
	Emeishan	Emeishan
	Mabian	Mabiandanxia
Luzhou	Naxi	Tianxiandong
		Huatianjiudi
	Hejiang	Fobao
		Bijiashan
	Yongxu	Huagaoxi
		Danshan
		Qingliangdong
	Malongtan	Dongwoxiagu
	Gulin	Huangjinglaolin
	Jiangyang	Fangshan
Zigong	Ziliujing	Feilongxia
	Rongxian	Jinhuasuoluogu

Methodology

Remote Sensing Dataset

The original operational land imager (OLI) and thermal infrared sensor (TIRS) images, encompassing the study area were acquired during the dry season on Mar 29th, 2019 (LC81280402019088LGN00), Apr 18th, 2018 (LC81290392018108LGN00 & LC81290402018108LGN00), and May 2nd, 2020 (LC08_L2SP_128039_20200502_20200820_02_T1) by the Landsat 8 satellite and were retrieved from the GSCloud platform (http://www.gscloud.cn/home). Each image includes one panchromatic band (band 8), eight multi-spectral bands (bands 1–7 and 9), and two thermal infrared bands (bands 10 and 11). The spatial resolution of band 8 is 15 m, and the multi-spectral bands have resolutions of 30 m. While the spatial resolutions of the infrared bands are originally 100 m, they were re-sampled to 30 m. The cloud content of the product is less than 1%. Additionally, alongside the OLI and TIRS images, twelve ASTER Global Digital Elevation Model (ASTER GDEM) images (N28-30E103-106) with a spatial resolution of 30 m covering the study area were downloaded from the GSCloud platform. Table 2 provides the essential details of these remote sensing data.

Terrain Analysis

The ENVI 5.3 software (https://www.nv5geospatialsoftware.com/Products/ENVI) was employed for terrain analysis. Initially, twelve ASTER GDEM images with a spatial resolution of 30 m were mosaicked to create a comprehensive image covering the entire study area. Subsequently, this composite image was utilized to compute slopes using the "Topographic Model" function. The resulting slopes were categorized into two groups: high-angle and low-angle, with a designated cutoff value of 40° (Qiu et al. 2015). The subset representing the high-angle group was then exported as a raster GeoTIFF file.

Regional Structural Interpretation

Faults and fractures were discerned by analyzing a remote sensing image, emphasizing alterations in rock units induced by displacement and deformation. In this investigation, structural separations were identified through the interpretation of Landsat 8 images using a specific band combination (Red, band 4; Green, band 3; Blue, band 2). The identification process relied on observable evidence, including variations in vegetation, deviations in stream paths, and abrupt lithological changes manifested as alterations in hues and textures within the images. The outcomes of this analysis were exported as a raster GeoTIFF file.

Field Investigation and Measurement of Joint Geometry

A field route survey was conducted on the Danxia landform sites enumerated in Table 1, wherein photographs and GPS locations of the sites were systematically captured and documented. The mechanical and kinematic properties of joints were assessed by interpreting field geological phenomena, including the distinctive features of joint planes. Geometry parameters such as dip and strike of the joints were measured using a geological compass and subsequently

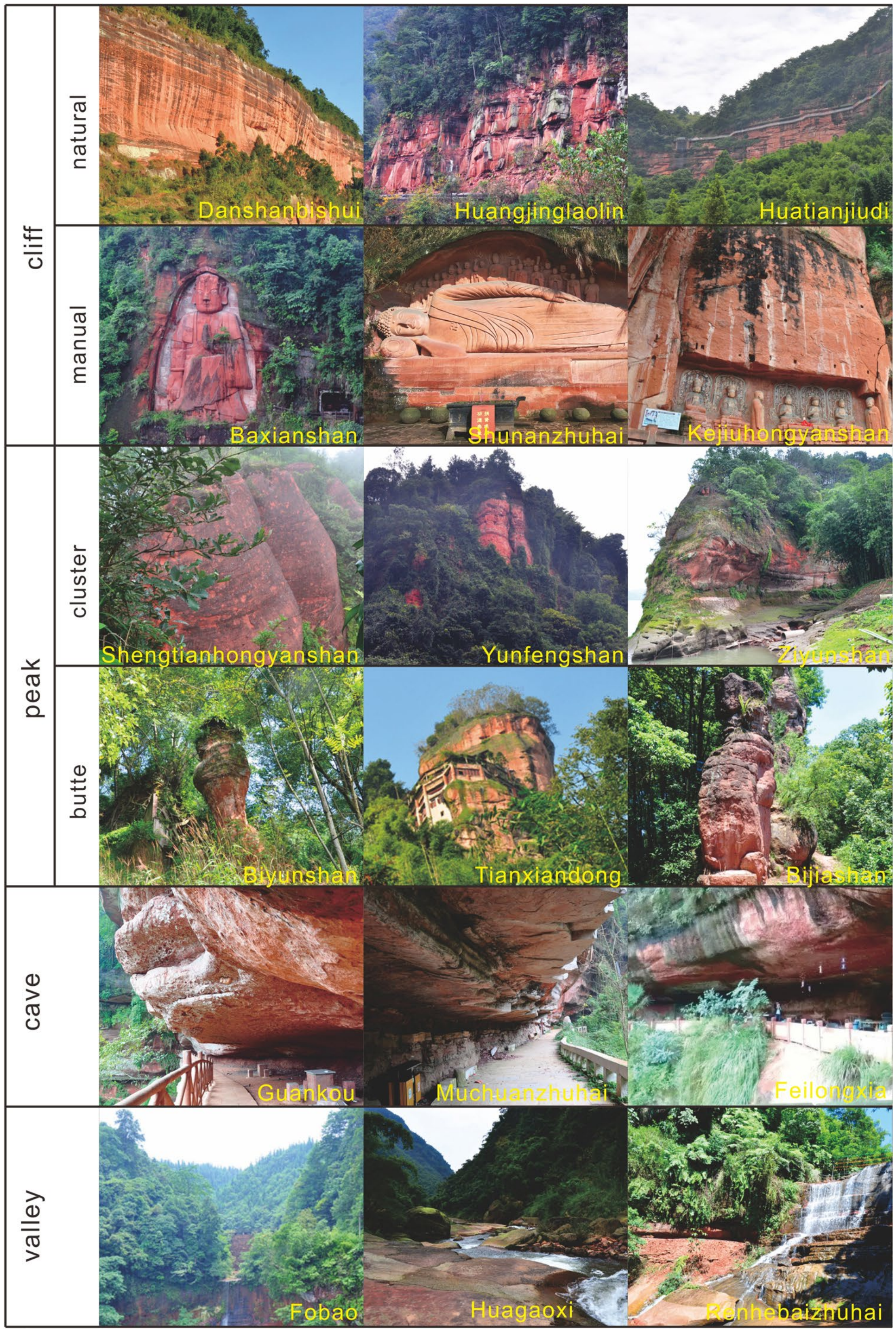

Fig. 3 Typical photographs showing different types of Danxia landforms in the southern Sichuan Basin

represented in stereographic projections through the CGDK (Qiu et al. 2013) add-in of CorelDRAW software (https://www.coreldraw.com/en/).

Results

Types and Distribution of Danxia Landforms

Based on a comprehensive field investigation covering approximately 150 sites (refer to Appendix Table 4) encompassing 35 Danxia landforms in the southern Sichuan Basin, a categorization of Danxia tourism resources into four

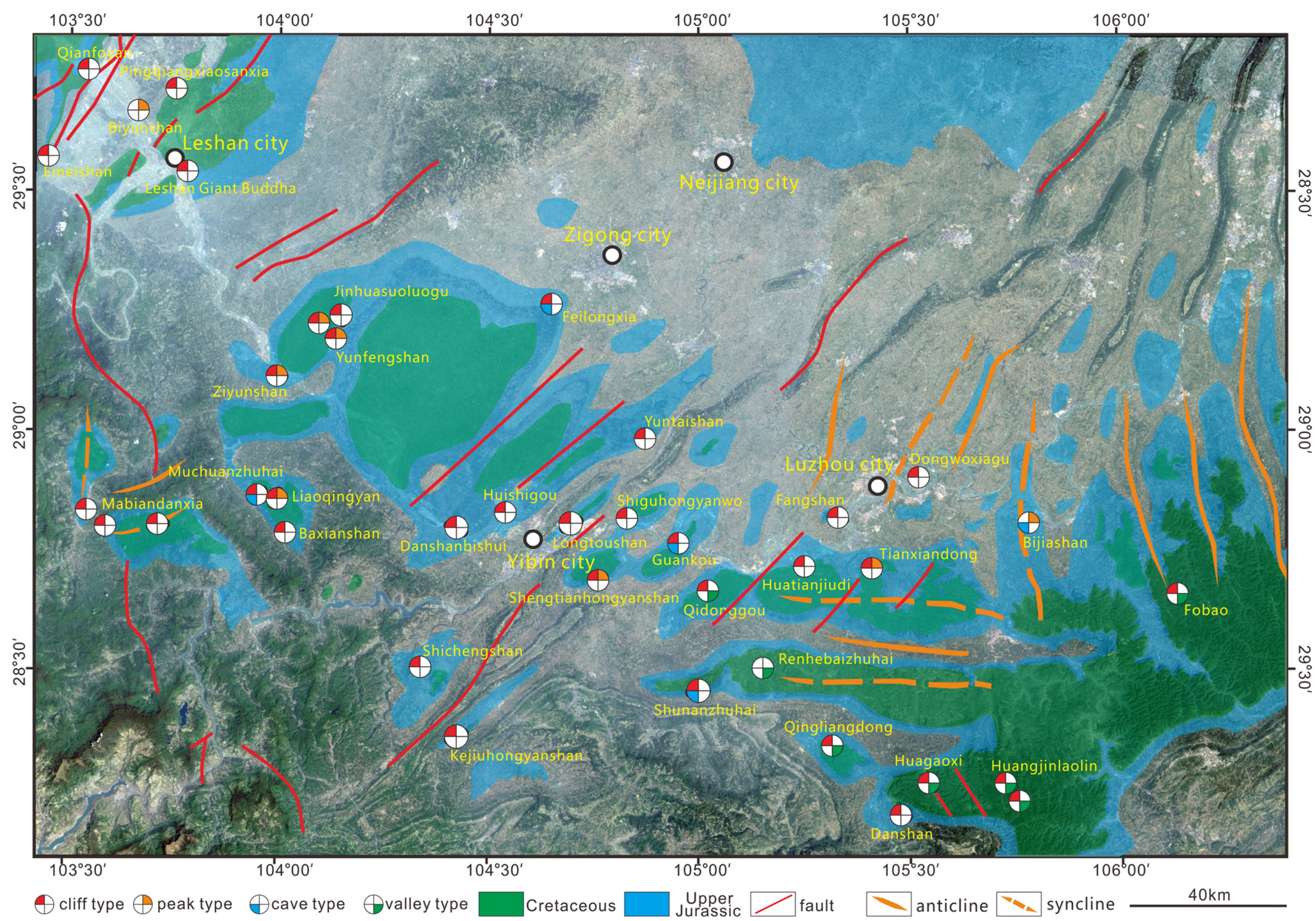

Fig. 4 Landsat8 truth color image showing distributions of different types of Danxia landforms, Late Jurassic, and Cretaceous red beds, regional faults, and folds

Table 2 Basic information about the remote sensing data used in this study

Data identifier	Data type	Acquision date	Bands (resolution)
LC81280402019088LGN00	Landsat 8	Mar 29th 2019	Bands 1–7 and 9 (30 m) Bands 8 (15 m) Bands 10 and 11 (100 m resampled to 30 m)
LC81290392018108LGN00		Apr 18th 2018	
LC81290402018108LGN00		Apr 18th 2018	
LC08_L2SP_128039_20200502_20200820_02_T1		May 2nd 2020	
N28E103	ASTER GDEM		30 m
N28E104			
N28E105			
N28E106			
N29E103			
N29E104			
N29E105			
N29E106			
N30E103			
N30E104			
N30E105			
N30E106			

distinct types based on their geometry characteristics has been identified. These types include (1) cliff type, (2) peak type, (3) cave type, and (4) valley type. The cliff type further comprises (1–1) natural cliff type and (1–2) manually modified cliff type. The natural cliff type is formed solely through geological processes, whereas the manually modified cliff type undergoes artificial alterations, such as cliff carvings and cliff architectures. The peak type is subdivided into (2–1) cluster type and (2–2) butte type. The cluster type may manifest as multiple peaks arranged in a line or a single peak with barrier-like characteristics, while the butte type is characterized by isolated single peak. Cave type is delineated by semi-closed caves developed along bedding planes. The valley type assumes a "V" shape, featuring red sandstone at the valley bottom often accompanied by a river. Illustrative photographs depicting various Danxia types are presented in Fig. 3. The occurrence and distribution of each Danxia type are itemized in Table 3 and graphically depicted in Fig. 4.

Distribution of Sedimentary Strata, Fold, and Fault

The results of structure interpretation based on remote sensing imagery were rigorously scrutinized through a

Table 3 Statistic table showing different types of Danxia landforms in southern Sichuan Basin

City	County	Name	Cliff		Peak		Cave	Valley
			Natural	Manual	Cluster	Butte		
Yibin	Changning	Shunanzhuhai	○	○			○	
		Qidonggou	○					○
	Gaoxian	Kejiuhongyanshan	○	○				
		Shengtianhongyanshan	○		○			
	Nanxi	Guankou	○				○	
		Yuntaishan	○					
	Cuiping	Danshanbishui	○	○				
		Shiguhongyanwo	○					
		Huishigou	○	○				
		Longtoushan	○					
	Jiangan	Renhebaizhuhai						○
	Pingshan	Baxianshan	○	○				
	Xuzhou	Shichengshan	○					
Leshan	Shizhong	Leshan Giant Buddha	○	○				
		Pingqiangxiaosanxia	○					
	Muchuan	Muchuanzhuhai	○				○	
		Liaoqingyan	○			○		
	Jiajiang	Qianfoyan	○	○				
		Biyunshan				○		
	Jianwei	Yunfengshan	○		○			
		Ziyunshan	○		○			
	Emeishan	Emeishan	○					
	Mabian	Mabiandanxia	○					
Luzhou	Naxi	Tianxiandong	○			○		
		Huatianjiudi	○					
	Hejiang	Fobao	○					○
		Bijiashan				○	○	
	Yongxu	Huagaoxi	○					○
		Danshan	○					
		Qingliangdong	○					○
	Malongtan	Dongwoxiagu	○					
	Gulin	Huangjinglaolin	○					○
	Jiangyang	Fangshan	○					
Zigong	Ziliujing	Feilongxia	○				○	
	Rongxian	Jinhuasuoluogu	○					
Total number			32	6	3	4	5	6

comparative analysis with the structural map and geological map of Sichuan Province, along with on-site field verification. The validated outcomes are illustrated in Fig. 4. The fold structures identified exhibit trending directions categorized into E-W, N-S, NE-SW, NNE-SSW, and NNW-SSE groups, determined by the axial surfaces of these structures. Concurrently, the fault structures predominantly trend in NE-SW and NNE-SSW directions, with secondary orientations observed in NW–SE and N-S directions. Given that Danxia landforms are typically associated with Upper Jurassic and Cretaceous Formations, the stratigraphic distribution is also presented in Fig. 4. Notably, the Cretaceous strata are predominantly situated along the periphery of the basin, whereas Upper Jurassic formations are concentrated in the central region of the basin.

Topographic and Geomorphic Features

The outcomes of the digital elevation model and slope analysis are presented in Fig. 5. Evidently, there is a gradual decrease in altitude from the edge of the basin towards the interior. Altitude changes facilitate the classification of three distinct regions: the mountain region, transition region, and plain region. The mountain region is characterized by elevated altitudes, while the plain region exhibits lower altitudes. Notably, all 35 identified Danxia landforms are situated in the mountain and transition regions, with none in the plain region. Regardless of whether it is the mountain or transition region, the known Danxia landforms are consistently associated with areas characterized by steep slopes. Specifically, in the transition region, viable Danxia landforms can still develop in areas with steep slopes, even if the altitudes of such areas are not exceptionally high.

Geometry of Joint

In the “Topographic and Geomorphic Features” section, remote sensing and GIS technologies were employed to identify regional folds and faults, crucial for comprehending the stress field within the southern Sichuan Basin. Alongside these structures, joints offer valuable insights into the stress field based on rock shear criteria. Given that joints cannot be directly identified on remote sensing imagery, we conducted field investigations to measure the geometry of joints in red sandstones, as illustrated in Fig. 6a and c. This exploration revealed the presence of two distinct groups of conjugate shearing joints. The first group encompasses joints with azimuths ranging from 310 to 335° and dip angles within the range of 63 to 72°, as well as joints with azimuths between 172 and 181° and

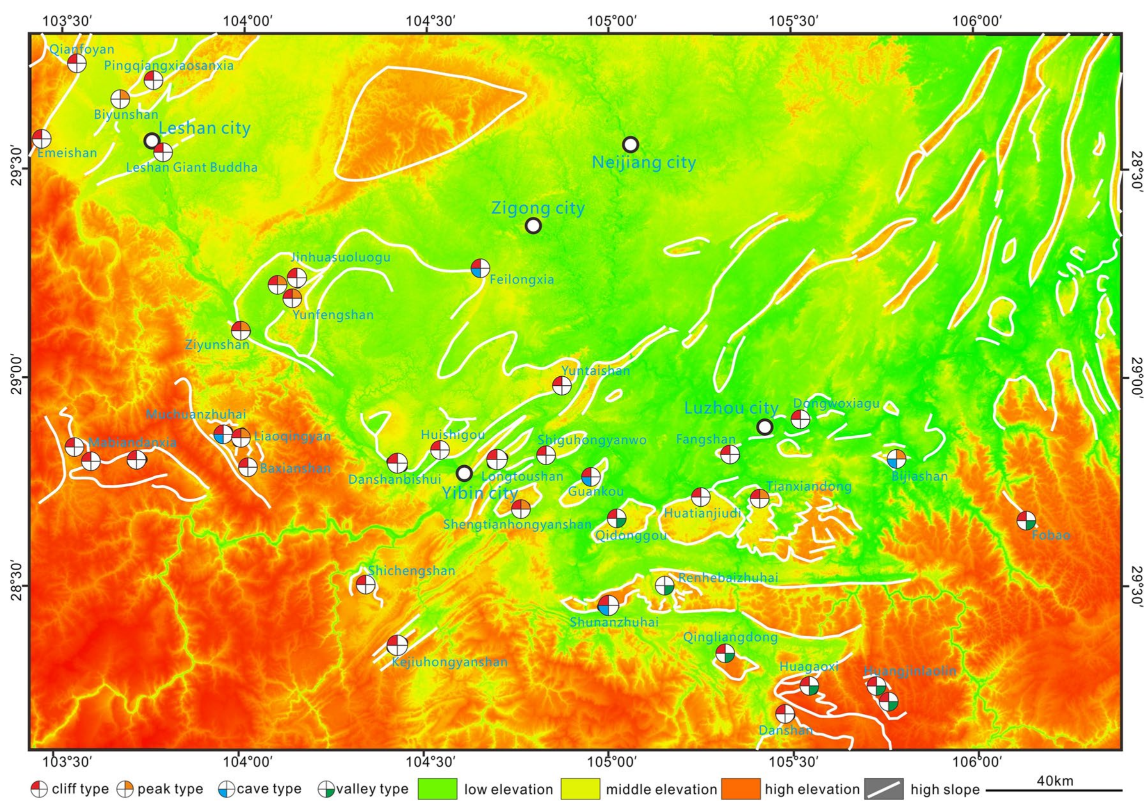

Fig. 5 Topographic map showing different types of Danxia landforms and areas with steep slopes

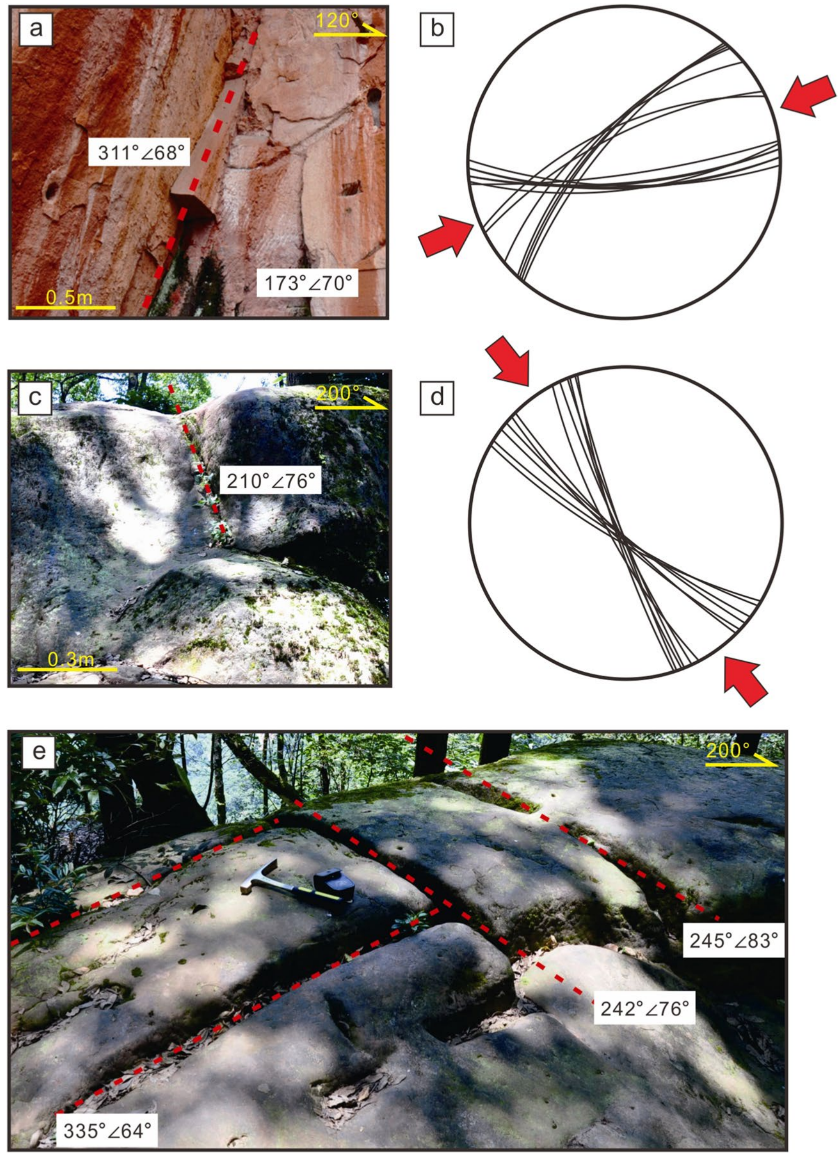

Fig. 6 **a** and **c** Diamond conjugate shear joints; **b** and **d** stereographic projections of conjugate shear joints; **e** chessboard-like joints, of which the 335°/64°group was cut by the 242°/76°group

dip angles spanning from 70 to 81° (Fig. 6b). The second group includes joints characterized by azimuths ranging from 210 to 225° and dip angles from 76 to 82°, alongside joints with azimuths spanning from 242 to 252° and dip angles ranging from 76 to 85° (Fig. 6d). Notably, the first group is intersected by the second group, as depicted in Fig. 6e, suggesting that the second group formed subsequent to the formation of the first group.

Discussion

The Interplay of Danxia Landforms with Strata, Topography, and Structure

Danxia, a distinctive landform, emerges through the erosion of red beds primarily composed of terrigenous clastic rocks such as mudstone, sandstone, and conglomerate. In the southern Sichuan Basin, Danxia landforms are intricately linked to Late Jurassic to Cretaceous red beds, with 21 landforms associated with the former and 29 with the latter (Fig. 7a). This study categorizes Danxia landforms into four types: cliff, peak, cave, and valley. The distribution includes 32 landforms for the cliff type, 7 for the peak type, 6 for the valley type, and 5 for the cave type. Altitudinally, 26 Danxia landforms are situated between 400

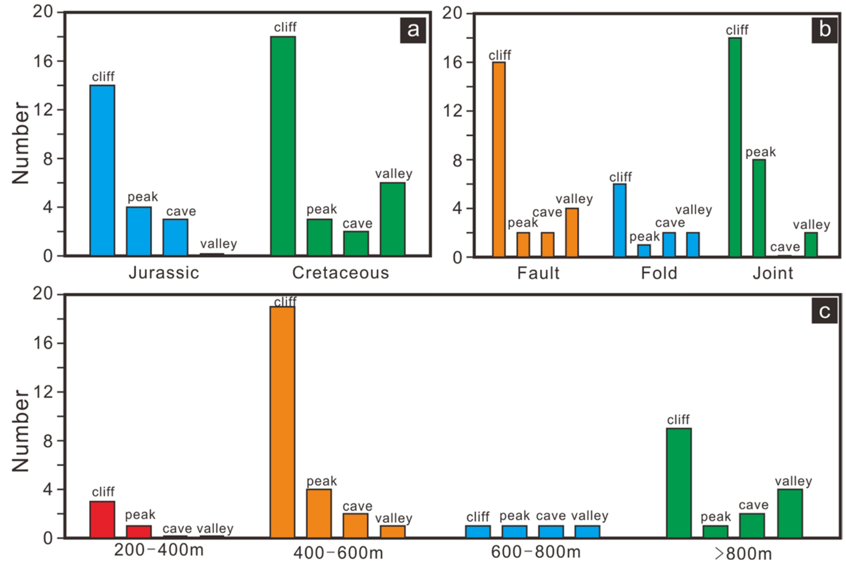

Fig. 7 Statistic results showing the relationships between different types of Danxia landforms and **a** the Late Jurassic and Cretaceous red bed **b** fault, fold and joint structure **c** different altitudes

and 600 m above sea level, 16 above 800 m, 4 between 200 and 400 m, and the remaining 4 between 600 and 800 m (Fig. 7c). Remarkably, all valley-type Danxia landforms are developed in Cretaceous strata, predominantly positioned above 800 m sea level, with two exceptions located between 400 and 800 m. In contrast, the other three types manifest in both Late Jurassic and Cretaceous strata across all altitudes without specificity. Furthermore, the majority of Danxia landforms are situated in areas with steep slopes (Fig. 5), where fractures, folds, and joints are well developed (Figs. 4, 6). Notably, the formation of Danxia landforms is intricately tied to geological structures. For instance, many cliffs and peaks align with or are intersected by joints and faults, while certain cliffs emerge at the uplifting terminations of folds. Additionally, lateral erosion of water flow can give rise to caves within cliffs.

Peng et al. (2013) proposed a model delineating the evolutionary stages of Danxia landforms, encompassing six phases: Early Youth, Late Youth, Early Adulthood, Late Adulthood, Early Decline, and Late Decline. However, a contrasting viewpoint was presented by Zhang et al. (2018), contending that the Danxia Mountain, representative of the Late Adulthood stage, is older than the Jianglang Mountain, typifying the Late Decline stage. Notably, prior studies (Liu et al. 2021a, b) highlight a surface denudation of 1.5–4.0 km in the south Sichuan Basin during the Cenozoic, with varying degrees of denudation observed in specific regions such as Leshan, Zigong, Neijiang, Yibin, and Luzhou (ranging from 1.5 to 3.5 km). This suggests a gradually diminishing denudation trend. Nevertheless, a paradox emerges as the Danxia landforms in Leshan and Yibin exhibit notable similarities, contrary to the distinctions proposed by Peng et al. (2013). Furthermore, despite comparable denudation levels in Yibin and Luzhou, the prevalence of valley-type Danxia landforms is more pronounced in Luzhou, situated at a higher altitude than Yibin. Consequently, the applicability of the model proposed by Peng et al. (2013) appears constrained to specific Danxia instances and may not universally hold across different locations. The diverse initial conditions and evolutionary environments present in distinct places underscore the need for a nuanced understanding of Danxia landform evolution.

Interconnection of Danxia Development and Tethys Evolution

The Danxia landforms in the South Sichuan Basin are intricately tied to Late Jurassic to Cretaceous strata. In the Late Jurassic period, the northeastern margin of the Yangtze Craton and the western Jiangnan Orogen experienced uplift and denudation due to the combined effects of southward thrusting of the Qinling Orogen (e.g., Yan et al. 2018), and the northwestward expansion of the Jiangnan Orogen and Chuanexiang fold-thrust belt (e.g., Yan et al. 2003; Li et al. 2014; Qiu et al. 2016). This led to extensive fluvial–deltaic–lacustrine depositions across the northern, eastern, southern, and central Sichuan Basin (Guo et al. 1996; Wang and Xu 2001; Liu et al. 2005, 2010). During the Early Cretaceous, the intra-cratonic depression of the Sichuan Basin subsided westward, resulting in fluviolacustrine depositions along the west and southwest sides of the basin (Li et al. 2018). Subsequently, in the Late Cretaceous, continuous compression from the Qinling Orogen uplifted and denuded the northern Sichuan Basin rapidly. Sediments from the Songpan-Ganzi terrane, the Longmenshan thrust belt, and the uplifted areas of the northern and northeastern Sichuan Basin were transported and deposited in the south and southwest sides of the basin (e.g., Yan et al. 2011; Cook et al. 2013; Li et al. 2018). The red beds formed by the aforementioned Jurassic and Cretaceous deposits provided the material foundation for the subsequent formation of Danxia landforms.

It is noteworthy that the Danxia landforms in the South Sichuan Basin are influenced by faults, folds, and joints. The fold structures are categorized into E-W, N-S, NE-SW, NNE-SSW, and NNW-SSE groups (Fig. 4), among which the E-W and NE-SW groups indicate maximum compressive stresses in the directions of N-S and NW–SE, while the N-S, NNE-SSW, and NNW-SSE groups indicate a sub-E-W maximum compressive stress. Fault structures, including N-S and NE-SW reversed faults (Fig. 4), suggest maximum compressive stresses in the directions of E-W and NW–SE. The age of the youngest deformed or broken rock associated with these structures suggests their formation in the Cenozoic era, indicating changes in the tectonic stress field during this period.

Guo and Dong (2019) reported the shear failure angle of ~ 22° for sandstone, namely only diamond conjugate shear joints can be observed in sandstone for the same tectonic stress field. Field investigations reveal two groups of conjugate shear joints (Fig. 6), one indicating a sub-E-W maximum compressive stress (Fig. 6b) and the other representing a NW–SE maximum compressive stress (Fig. 6d). The cross-cut relationship between these two groups (Fig. 6e) implies a change in the direction of maximum compressive stress during the Cenozoic, aligning with the proposed tectonic events by Wang et al. (2014). This shift, from sub-E-W compression related to the eastward expansion of the Tibetan Plateau (25–30 Ma) to NW–SE compression associated with the southeastward extrusion of the Chuandian fragment (12.8–15.4 Ma), underscores the dynamic tectonic evolution of the region.

Usually, red beds need uplift and suffer erosion to generate different types of Danxia landforms. It is generally accepted that the south Sichuan Basin weakly deformed during the Late Mesozoic but uplifted mainly in the Cenozoic. Deng et al. (2014) reported the apatite fission-track thermal history simulation results that reveal a relatively slow exhumation rate of ~ 0.15 mm/year during ~ 30 to ~ 10 Ma and a relatively rapid exhumation rate of ~ 0.4 to 0.8 mm/year since ~ 10 Ma for Daliangshan fold belt. An et al. (2008) yielded the fission track dating results for the Mabian area, southwest Sichuan basin, indicating an extensive tectonic uplift occurred since ~ 3 Ma. These apatite fission-track results further suggest a multi-stage tectonic event driven by the eastward growth of the Tibetan Plateau, during which Jurassic and Cretaceous red beds in the south Sichuan basin uplifted and exposed to the surface and suffered erosion, a situation that benefits Danxia landform formation.

Implications for Spatial Distribution of Danxia Landforms

As depicted in Fig. 8, two prominent tectonic domains shaped China from the Mesozoic to the Cenozoic: the Tethys-Himalayan tectonic domain and the Paleo-Pacific tectonic domain. Notably, the spatial distribution of Danxia landforms in the Sichuan Basin and Qilian-Liupan regions is closely linked to the Tethys-Himalayan tectonic domain, while those in the South China Region are associated with the Paleo-Pacific tectonic domain. Expanding on the discussions in the "The Interplay of Danxia Landforms with Strata, Topography, and Structure" section and the "Interconnection

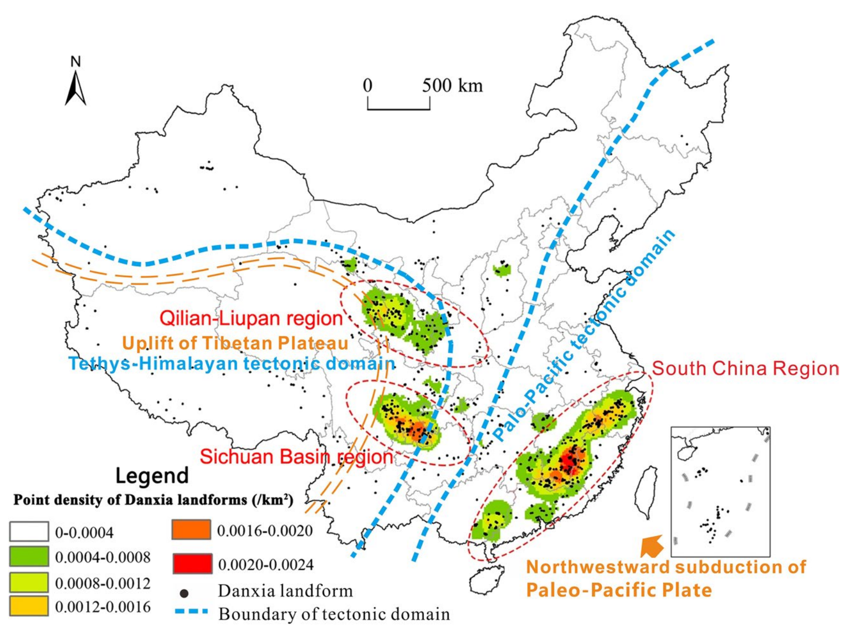

Fig. 8 Distribution of Danxia landforms with tectonic domains in China (modified after Yan et al. 2019; Qiu et al. 2022)

of Danxia Development and Tethys Evolution" section, the formation of Danxia landforms in the Sichuan Basin is genetically controlled by the periphery of the Tethys-Himalayan tectonic domain, characterized by active sedimentary and tectonic processes. This region provided the essential material, structural, and erosional foundations for the development of Danxia landforms. Similarly, the Danxia landforms in the Qilian-Liupan region also emerged along the edge of the Tethys-Himalayan tectonic domain, mirroring the conditions observed in the Sichuan Basin Region. Previous studies have established a connection between Danxia landforms in the Qilian-Liupan region and Jurassic to Cretaceous red beds formed during the uplift of the Tibetan Plateau (e.g., Zhang 2020; Ding et al. 2014a, 2014b). It is noteworthy that the Danxia landforms in the South China Region deviate from the edge of the Tethys-Himalayan tectonic domain; instead, they situate within the NE-SW trending structural belt forged by the northwestward subduction of the Paleo-Pacific Plate. Unlike their counterparts in other regions, the Danxia landforms in the South China Region are controlled by joints and faults oriented in NNW and NE directions (Lu 2014; Guo et al. 2023), aligning with the NW–SE compression (Jiang et al. 2013; Chen et al. 2019). Therefore, the distinct distribution characteristics of Danxia landforms across these regions are direct outcomes of the evolutionary trajectories of the respective tectonic domains.

Conclusions

(1) Four distinct types of Danxia landforms—cliff, peak, cave, and valley—were meticulously observed and classified in the southern Sichuan Basin. Notably, all these types exhibit a clear preference for locations characterized by steep slopes. The valley type, specifically, tends to manifest in areas with elevated altitudes, while the other types do not display a discernible preference for specific altitude ranges.
(2) The genesis of Danxia landforms is intricately linked to red beds deposited during the Late Jurassic to Cretaceous periods. These landforms are influenced by faults, folds, and joints that materialized during the Cenozoic era. Additionally, the Cenozoic uplift played a pivotal role in initiating a rapid denudation process of red beds, significantly contributing to the formation of Danxia landforms.
(3) The evolution of the Tethys-Himalayan tectonic domain since the late Jurassic laid the groundwork for the material and structural aspects of Danxia landforms in the southern Sichuan Basin. This tectonic evolution exerted a considerable influence on the overall formation and progression of these unique landforms.
(4) The distinctive distribution patterns of Danxia landforms are direct outcomes of the tectonic evolution. Notably, Danxia landforms within the same tectonic domain may be genetically related, sharing a common dynamic background that shapes their unique characteristics and features.

Supplementary Information The online version contains supplementary material available at https://doi.org/10.1007/s12371-024-00928-y.

Author Contribution Jun-Ting Qiu summarized the results and wrote this paper. Hong-Xu Mu downloaded and processed the remote-sensing images. Xin-Min Rui and Yan-Jie Yang did the structure and slope analyses. Pengju Li and Liang Qiu carried out the field work and took photos of Danxia heritages. Chao-Bin Xu did the Danxia classification.

Funding NSFC (no. 42030306).

HNKF project of State Administration of Science, Technology and Industry for National Defence, PRC (no. YH2001).

Data Availability All data or data source are incorporated or mentioned in the article and its online supplementary material.

Declarations

Conflict of Interest The authors declare no competing interests.

References

Brocx M, Semeniuk V (2007) Geoheritage and geoconservation- history, definition, scope and scale. J R Soc West Aust 90:53–87
An YF, Han ZJ, Wan JL (2008) Fission track dating of the Cenozoic uplift in Mabian area, southern Sichuan Province, China. Sci China Ser D: Earth Sci 51:1238–1247
Chen DJ (1984) Natural red stone park—Danxia Mountain. Guangdong Gardens 2:54–56
Chen TG, Zhu JB, Wang QN, Yan HT, Liu YQ, Guan DW (2019) Geological characteristics and genesis analysis of the Ningdu Danxia landform in southern Jiangxi Province. East China Geol 40(01):27–34 (In Chinese with English abstract)
Chen L, Shi Y, Ng Y et al (2022) Roles of algae in honeycomb weathering in humid climate: an example from Danxiashan UNESCO Global Geopark of China. Geoheritage 14:120
Cook KL, Royden LH, Burchfiel BC, Lee YH, Tan X (2013) Constraints on Cenozoic tectonics in the southwestern Longmen Shan from low-temperature thermochronology. Lithosphere 5(4):393–406
Deng J, Wang QF, Li GJ, Li CS, Wang CM (2014) Tethys tectonic evolution and its bearing on the distribution of important mineral deposits in the Sanjiang region, SW China. Gondwana Res 26:419–437
Ding HW, Wang SY, Yi Z, Yao XR, Meng JH, Zhang XR (2014a) Geologic origins of Danxia and colorful hills of Zhangye and comparison with Danxia landform in southern China. Arid Land Geogr 37(03):419–428 (In Chinese with English abstract)
Ding HW, Wang SY, Yao XR, Kang L, Yi Z, Zhang XR (2014) The geologic origins of Danxia and colorful hills landform of Zhangye in China. Gansu Geol 23(02):70–77 (In Chinese with English abstract)
Dong YP, Zhang GW, Hauzenberger C, Neubauer F, Yang Z, Liu XM (2011) Paleozoic tectonics and evolutionary history of the Qinling

orogen: evidence from geochemistry and geochronology of ophiolite and related volcanic rocks. Lithos 122:39–56

Guo Z-W, Deng K-L, Han Y-H, Liu Y-K, Yin J-T, Wang Q-G, Liang E-Y, Li G-J, Chen Z-G, Liu Z-Z (1996) The formation and development of Sichuan Basin. Geological Publishing House, Beijing

Guo B, Dong H (2019) Shear failure modes and AE characteristics of sandstone and marble fractures. Open Geosci 11:249–262

Guo J-Q, You Z-P, Zhao Y-N (2008) A study of geoheritage regionalization in Sichuan. Acta Geol Sichuan 28(4):327–330 (In Chinese with English Abstract)

Guo FS, Lin YY, Chen LQ, Zhou WP, Li HW, Chen LK, Wu ZC, Li GR, Guo Z, Li B (2023) A study on the landform landscape control factors and landscape types of Danxia Mountain World Geopark. Geosciences, (in press) https://doi.org/10.19657/j.geoscience.1000-8527.2023.099

Jia D, Wei G, Chen Z, Li B, Zeng Q, Yang G (2006) Longmen Shan fold-thrust belt and its relation to the western Sichuan Basin in central China: new insights from hydrocarbon exploration. AAPG Bull 90(9):1425–1447

Jia Z, Wu F, Hou D (2023) Geodiversity, geotourism, geoconservation, and sustainable development in Longyan Aspiring Geopark (China). Geoheritage 15:11

Jiang YB, Guo FS, Hu ZH, Sun CM, Liu LQ, Huang BH (2009) A study on the features of Danxia landform in Longhushan World Geopark and comparing with others in China. J Mt Sci 27(03):353–360 (In Chinese with English abstract)

Jiang YB, Guo FS, Chen SS (2013) Spatial distribution and its genesis of the Danxia landforms in Xinjiang Basin Jiangxi. J Mt Sci 31(06):731–737 (In Chinese with English abstract)

Li X, He QC, Dong Y, Cao XJ, Wang ZY, Duan XM (2013) An analysis of characteristics and evolution of Danxia Landform in the South of Chishui County, Guizhou. Acta Geoscientia Sinica 34(04):501–508

Li J, Zhang Y, Dong S, Johnston ST (2014) Cretaceous tectonic evolution of South China: A preliminary synthesis. Earth Sci Rev 134:98–136

Li Y, He D, Li D, Lu R, Fan C, Sun Y, Huang H (2018) Sedimentary provenance constraints on the Jurassic to Cretaceous paleogeography of Sichuan Basin, SW China. Gondwana Res 60:15–33

Li Q, Wu R, Ng Y (2022) Developing culturally effective strategies for Chinese to English geotourism translation by corpus-based interdisciplinary translation analysis. Geoheritage 14:6

Li XN, Jiang YB, Wang PP (2023) Features and genesis analysis of Danxia landscape in the northwest foothills of the Wuyi Mountains. East China Geol 44(02):228–238 (In Chinese with English abstract)

Liu SR (1986) Formation and application of the landform in north Guangdong Province. Acta Sci Natur Univ Sunyatseni 25(1):57–64

Liu SR, Huang RH (1991) Redstone karst and Danxia landforms in Guangdong Province. Carsologica Sinica 10(3):16–22

Liu SF, Steel R, Zhang GW (2005) Mesozoic sedimentary basin development and tectonic implication, northern Yangtze Block, eastern China: Record of continent–continent collision. J Asian Earth Sci 25:9–27

Liu SF, Wang P, Hu MQ, Gao TJ, Wang K (2010) Evolution and geodynamic mechanism of basin–mountain systems in the northern margin of the Middle–Upper Yangtze. Earth Sci Front 17:14–26 (Chinese with English abstract)

Liu S, Deng B, Jansa L, Li Z, Sun W, Wang G, Luo Z, Yong Z (2018) Multi-stage basin development and hydrocarbon accumulations: a review of the Sichuan Basin at eastern margin of the Tibetan Plateau. J Earth Sci 29(2):307–325

Liu S, Yang Y, Deng B, Zhong Y, Wen L, Sun W, Li Z, Jansa L, Li J, Song J, Zhang X, Peng H (2021a) Tectonic evolution of the Sichuan Basin. Southwest China Earth-Sci Rev 213:103470

Liu S, Yang Y, Deng B, Zhong Y, Wen L, Sun W, Li Z, Jansa L, Li J, Song J, Zhang X (2021b) Tectonic evolution of the Sichuan Basin, southwest China. Earth Sci Rev 213:103470

Lu JY (2014) Analysis of geomorphological features of mount Longhu based on DEM. China University of Geosciences, Wuhan, China

Luo C, Wang F (2015) The Danxia landforms in Sichuan Basin and the Castles of Southern Song Dynasty for resistance against Mongolia. J Leshan Normal Univ 30:64–69 (In Chinese with English Abstract)

Meng QR, Zhang GW (2000) Geologic framework and tectonic evolution of the Qinling Orogen, Central China. Tectonophysics 323:183–196

Mu H, Yan DP, Qiu L, Yang WX, Kong RY, Gong LX, Li S (2019) Formation of the Late Triassic western Sichuan foreland basin of the Qinling Orogenic Belt, SW China: sedimentary and geochronological constraints from the Xujiahe Formation. J Asian Earth Sci 183:103938

Peng H (2000) A survey of the Danxia landform research in China. SciGeogr Sin 20(3):203–221

Peng H, Pan Z, Yan L, Scott S (2013) A review of the research on red beds and Danxia landform. Acta Geogr Sin 68(9):1170–1181 (In Chinese with English Abstract)

Peng XH, Wu H, Li YZ, Zhang Y, Zhu J, Dang C (2020) A preliminary study on the genetic mechanism of wavy Danxia landform in Longzhou, Jingbian Shaanxi Province. Acta Geosci Sinica 41(03):443–451 (In Chinese with English abstract)

Peng XH, Wu H, Zhang JL, Wang Y, Zhu J (2023) A study on the landscape characteristics and development evolution of typical Danxia landform in Yan'an. Acta Geoscientia Sinica, https://link.cnki.net/urlid/11.3474.P.20231129.1650.004 (In Press, In Chinese with English abstract)

Qiu J-T, Song W-J, Jiang C-X, Wu H, Raymond MD (2013) CGDK: an extensible CorelDRAW VBA program for geological drafting. Comput Geosci 51:34–48

Qiu J-T, Li P-J, Yu Z-F, Li P (2015) Petrology and spectroscopy studies on Danxia geoheritage in Southeast Sichuan area, China: implications for Danxia surveying and monitoring. Geoheritage 7:307–318

Qiu L, Yan DP, Tang SL, Wang Q, Yang WX, Tang X, Wang J (2016) Mesozoic geology of southwestern China: Indosinian foreland overthrusting and subsequent deformation. J Asian Earth Sci 122:91–105

Qiu L, Kong R, Yan DP, Sun MuHX, Sun W, S, Han Y, Li C, Zhang L, Cao F, Ariser S, (2022) Paleo-Pacific plate subduction on the eastern Asian margin: Insights from the Jurassic foreland system of the overriding plate. GSA Bull 134(9–10):2305–2320

Ren F (2009) A study on the genetic model of Danxia landform in Longhushan Geopark. China University of Geosciences (Beijing) (In Chinese with English abstract)

Roger F, Jolivet M, Malavielle J (2010) The tectonic evolution of the Songpan-Garzê (North Tibet) and adjacent areas from Proterozoic to Present: a synthesis. J Asian Earth Sci 39:254–269

Shi Z, Xin C, Liu H et al (2022) Geoheritage geomorphology of an alpine region in northwest China: introduction to the Yeliguan National Geopark. Geoheritage 14:61

Shu H, Zhang F, Liu P (2022) Study on the characteristics and utilization of the Danxia geoheritage in northwest China: implication on popularly scientific education and undergraduate teaching. Geoheritage 14:38

Sun M, Yin A, Yan D, Ren H, Mu H, Zhu L, Qiu L (2018) Role of pre-existing structures in controlling the Cenozoic tectonic evolution of the eastern Tibetan plateau: new insights from analogue experiments. Earth Planet Sci Lett 491:207–215

The World Heritage Committee (2010) Report of the decisions adopted by the world heritage committee at its 34th session. Brasilia, pp 163–165

Wang QZ (2021) Research on the landscape formation mechanism and vulnerability of Danxia landform in Youba Zhongdu. Chengdu University of Technology (In Chinese with English abstract), Southwest Sichuan

Wang YB, Xu HJ (2001) Relations between evolution of sedimentary cycles and tectonic uplift around Sichuan Basin from Jurassic to Early Cretaceous. Earth Scie – J China Univ Geosci 26(3):241–246 (in Chinese with English abstract)

Wang E, Meng K, Su Z, Meng Q, Chu JJ, Chen Z, Wang G, Shi X, Liang X (2014) Block rotation: tectonic response of the Sichuan basin to the southeastward growth of the Tibetan Plateau along the Xianshuihe-Xiaojiang fault. Tectonics 33:686–717

Xu JH, Wang YY, Lian XY, Feng L (2013) Development and protection of geological relic landscape resources in Zhangye Danxia Geopark. J Arid Land Resour Environ 27(09):198–204

Yan DP, Qiu L (2020) Geology of China and adjacent regions: an introduction. J Asian Earth Sci 203:104533

Yan DP, Zhou MF, Song HL, Wang XW, Malpas J (2003) Origin and tectonic significance of a Mesozoic multi-layer over-thrust system within the Yangtze Block (South China). Tectonophysics 361(3–4):239–254

Yan DP, Zhou Y, Qiu L, Wells ML, Mu H, Xu CG (2018) The Longmenshan tectonic complex and adjacent tectonic units in the eastern margin of the Tibetan Plateau: a review. J Asian Earth Sci 164:33–57

Yan L, Peng H, Zhang S (2019) The spatial patterns of red beds and Danxia landforms: implication for the formation factors–China. Sci Rep 9:1961

Yan, DP, Zhou MF, Li SB, Wei GQ (2011) Structural and geochronological constraints on the Mesozoic-Cenozoic tectonic evolution of the Longmen Shan thrust belt, eastern Tibetan Plateau. Tectonics 30(6)

Yang L, Chen LQ, Pan ZX, Shao CJ, Wu H (2023) Characteristics and genesis of loess-covered Danxia landscape in Northern Shaanxi Province of China. J Mt Sci 41(4):508–520 (In Chinese with English abstract)

Zhang HW (2020) The lithological characteristics of the Zhangye red layer and the genesis of the Danxia landform. Lanzhou University, Gansu, China

Zhang G, Chen K, Zhang H, Zhang H (2018) The evolution stage decision of Danxia landform based on digital elevation model (DEM). Acta Sci Natur Univ Sunyatseni 57(2):12–21

Zhang P, Chen LQ, Shao CJ, Li W, Du DD (2023) Analysis of the landform characteristics and genesis of Danxia in the Wensu Grand Canyon of Aksu. Arid Land Geography (In Press, In Chinese with English abstract), Xinjiang

Zhu C, Peng H, Li ZX, Yu JB, Li L, Zhang GS, Zhu GY, Ouyang J, Zhong YS, Zhu Q, Zhou SQ, Zhen CG, Zhou RL, Li D, Zhu YM, Lv W, Wu HL (2009) Age and genesis of the Danxia landform on Jianglang Mountain Zhejiang Province. Acta Geosci Sinica 64(01):21–32 (In Chinese with English abstract)

Zhu C, Peng H, Ouyang J, Hu Z, Li L (2010) Rock resistance and the development of horizontal grooves on Danxia slopes. Geomorphology 123(1–2):84–96